Mechanisms in knockout reactions

D. Bazin,[1,*] R. J. Charity,[2] R. T. de Souza,[3] M. A. Famiano,[4,1] A. Gade,[1,5] V. Henzl,[1] D. Henzlova,[1] S. Hudan,[3] J. Lee,[1] S. Lukyanov,[6,1] W. G. Lynch,[1,5] S. McDaniel,[1] M. Mocko,[7,1] A. Obertelli,[8,1] A. M. Rogers,[1] L. G. Sobotka,[2] J. R. Terry,[9,1] J. A. Tostevin,[10,1] M. B. Tsang,[1] and M. S. Wallace[7,1]

[1]*National Superconducting Cyclotron Laboratory, Michigan State University, East Lansing, MI 48824, USA*
[2]*Department of Chemistry, Washington University, St. Louis, MO 63130, USA*
[3]*Department of Chemistry, Indiana University, Bloomington, IN 47405, USA*
[4]*Department of Physics, Western Michigan University, Kalamazoo, MI 49008, USA*
[5]*Department of Physics and Astronomy, Michigan State University, East Lansing, MI 48824, USA*
[6]*FLNR/JINR, 141980 Dubna, Moscow region, Russia*
[7]*Los Alamos National Laboratory, Los Alamos NM 87545, USA*
[8]*DAPNIA/SPhN, CEA Saclay, F-91191 Gif-sur-Yvette Cedex, France*
[9]*Department of Physics, Yale University, New Haven, CT 06520, USA*
[10]*Department of Physics, University of Surrey, Guildford GU2 7XH, UK*

(Dated: May 9, 2009)

We report the first detailed study of the relative importance of the stripping and diffraction mechanisms involved in nucleon knockout reactions, by the use of a coincidence measurement of the residue and fast proton following one-proton knockout reactions. The measurements used the S800 spectrograph in combination with the HiRA detector array at the NSCL. Results for the reactions ^{9}Be(^{9}C,^{8}B+X)Y and ^{9}Be(^{8}B,^{7}Be+X)Y are presented and compared with theoretical predictions for the two reaction mechanisms calculated using the eikonal model. The data show a clear distinction between the stripping and diffraction mechanisms and the measured relative proportions are very well reproduced by the reaction theory. This agreement adds support to the results of knockout reaction analyses and their applications to the spectroscopy of rare isotopes.

PACS numbers: 24.50.+g, 25.60.-t , 25.60.Gc, 25.60.Dz

In a nucleon knockout reaction, a single nucleon is removed from a fast moving projectile in a high energy collision with a light nuclear target. This type of reaction is being used extensively to probe the wave functions of rare isotopes produced at fragmentation facilities [1]. The success of this technique relies on the utilization of fast radioactive beams, which on one hand provide a high luminosity due to the use of thick targets, and on the other hand enables simple assumptions, such as the sudden and eikonal approximations, in the reaction theory. This unique combination has already yielded a significant amount of spectroscopic information on nuclei far from stability, where benchmarks of nuclear models such as the shell model are crucial.

Typical experiments employ thick targets, for luminosity, and γ-ray spectroscopy, but the removed nucleon is not detected. Since no information is recorded experimentally on the fate of the removed nucleon or the final state of the target nucleus, the reaction theory is used to estimate both the elastic (also called diffraction) and inelastic (also called stripping) nucleon removal mechanisms. These incoherent contributions to the knockout cross section are then summed before comparison with experiment. It is therefore of great importance to investigate the proportion of each reaction mechanism experimentally in order to validate the reaction theory, and assess any deviations due to approximations in the reaction dynamics. In particular, no experimental data showing the kinematics differences between the two mechanisms has been available so far.

More exclusive experiments, where the momentum vectors of both the heavy residue and removed nucleon are measured, are necessary to distinguish between the two reaction mechanisms. Several such exclusive experiments of nucleon removal reactions have been performed over a range of energies, e.g. [2–6]. However, most of these experiments have looked exclusively at the diffractive component of the cross section, either by design, due to the chosen acceptance of the detector system [2, 5], or by neglect of the stripping component based on calculations of the expected kinematics [7]. Other exclusive experiments with larger angular coverage for detection the removed nucleon [6, 8] did not report any observed kinematical differences between the stripping and diffraction mechanisms, the subject of this work.

The one-proton knockout reactions from ^{9}C and ^{8}B were chosen for several reasons, summarized in Table I. The diffraction component in the proton knockout from ^{8}B should be enhanced in comparison to ^{9}C due to its lower separation energy. The final states of both heavy residues are also well defined since ^{8}B has no bound excited state and ^{7}Be has only one. Finally, the possibility of producing a radioactive beam containing both nuclei, as well as the easier detection of the knocked out protons rather than neutrons, were further motivations. The eikonal calculations used the proton bound state and target and residue density parameters taken from previous studies [9]. The Coulomb breakup cross sections are also

included since these contribute to the diffractive components.

The experiment was carried out at the National Superconducting Cyclotron Laboratory (NSCL), where a primary beam of ^{16}O at 150 MeV/u was used to produce the ^{9}C and ^{8}B radioactive beams via projectile fragmentation on a 1763 mg/cm^2 ^{9}Be target. Both ^{9}C and ^{8}B beams were filtered out simultaneously by the A1900 fragment separator [10], and contained a small amount of ^{7}Be and ^{6}Li contamination. Reactions from the different components of this cocktail beam could be easily identified event-by-event using the time-of-flight measured between two plastic scintillators located in the beam line before the reaction target. The one-proton knockout reactions took place in the scattering chamber of the S800 spectrograph [11], on a 188 mg/cm^2 ^{9}Be target surrounded by the HiRA detector array [12]. The mid-target energies of the ^{9}C and ^{8}B beams were 97.9 MeV/u and 86.7 MeV/u, respectively. The one-proton knockout residues were collected and identified around 0° by the S800 spectrograph, whereas the light particles emerging at large angles were detected and identified by the HiRA array. The angles covered ranged from 11° to 60°. Due to the finite 5% momentum acceptance of the S800 spectrograph, several overlapping magnetic rigidity settings were necessary to cover the range of momenta spanned by the ^{8}B and ^{7}Be reaction residues.

The light-particle identification in the HiRA telescopes was performed using the signals from the silicon detector for energy loss versus the CsI crystal for total energy. The punch-through energy for protons in the CsI detector is around 120 MeV. From both reactions, events in coincidence with the one-proton knockout residues revealed not only protons, but deuterons and also a few tritons. Such deuteron and triton events must involve an inelastic interaction with the target. For events in coincidence with protons however, both elastic and inelastic interactions with the target are possible, corresponding to the diffraction and stripping mechanisms. To investigate the differences between these mechanisms experimentally, the energy of the detected proton was plotted versus that of the heavy residue, after proper calibrations of both the S800 spectrograph and the HiRA array. The energy of the heavy residue is reconstructed from the focal-plane positions and angles measurements via an inverse map calculated with the ion optics program COSY Infinity [16]. The resulting spectra are shown in Fig. 1, where a narrow band at high energy can be observed for both reactions. This narrow band corresponds to events in which there is minimal transfer of energy to the target and the incoming projectile kinetic energy is essentially shared between the heavy residue and the proton. These events are classified as due to elastic breakup. In contrast, the events located below this band correspond to reactions where a large portion of the initial kinetic energy of the projectile is lost to the target nucleons. These

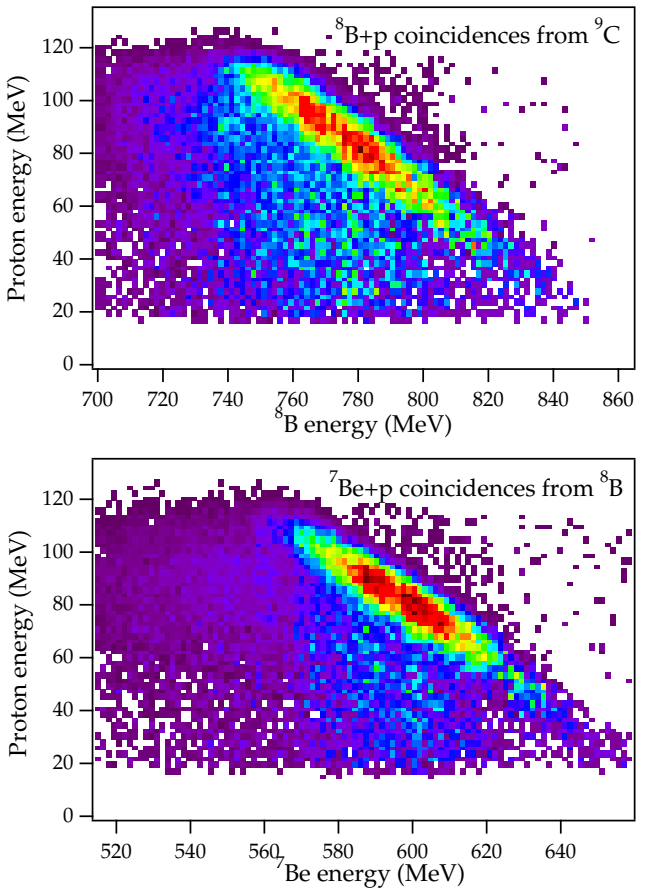

FIG. 1: (color online) Two dimensional spectra of the energy of protons and of the heavy residue in one-proton knockout reactions from ^{9}C (top) and ^{8}B (bottom) projectiles, respectively. The narrow bands of constant energy sum correspond to elastic breakup whereas other events are associated with inelastic breakup (see text). The small fluctuations in number of counts are due to the way the spectra were produced, by adding the data from the various magnetic rigidity settings used during the experiment.

events are identified as inelastic breakup since they involve excitation of the target.

To further characterize the two classes of events observed in the previous spectra, the energy sum spectra of the heavy residue and light particle detected in coincidence was reconstructed from individual energies. They are shown in Fig. 2 for all coincidence events, as well as for protons only and deuterons only. The events in coincidence with protons show two distinct features: a sharp peak at high energy and a broad, overlapping peak at lower energy. For events in coincidence with deuterons on the other hand, only the broad peak is visible. Since the neutron in the deuteron can only originate from the target, this further indicates that the sharp peak corresponds to elastic breakup processes, where the target remains in its ground state. The width of the elastic peak arises from both the momentum width of the incoming

TABLE I: The stripping and diffraction components of the one-proton knockout cross section for ^{9}C and ^{8}B are calculated in the eikonal model. The small contributions from Coulomb breakup are taken from [14], which used very similar incident energies. The spectroscopic factors C^2S_{SM} are taken from shell-model calculations using the PJT interaction [15]. The radial mismatch factor M for the ^{9}C case arises from the imperfect overlap of the least bound proton wave function in the ^{8}B residue and the ^{9}C projectile, as calculated in [14]. The $\%_{diff}$ column indicates the predicted proportion of diffraction cross section (including Coulomb) relative to the total. The last 4 columns show the predicted stripping and diffraction cross sections normalized to the inclusive experimental cross section, as well as the experimental results.

Initial state	Final state	S_p (MeV)	σ_{str} (mb)	σ_{diff} (mb)	σ_C (mb)	C^2S_{SM}	M	$\%_{diff}$	σ_{str}^{pred} (mb)	σ_{diff}^{pred} (mb)	σ_{str}^{exp} (mb)	σ_{diff}^{exp} (mb)
^{9}C	^{8}B	1.296	44.57	15.27	1.1	0.94	0.976	26.8	41.0	15.0	42(3)	14(2)
^{8}B	^{7}Be$_{gs}$	0.137	64.42	31.65	7.7	1.036	1	37.1	79.9	47.1	79(7)	48(6)
^{8}B	^{7}Be$_{ex}$	0.566	57.34	24.44	3.4	0.22	1					

beam (1%), and the broadening due to the differential energy loss in the target - the energy difference between reactions happening at the front and the back of the target.

In order to evaluate the proportion of elastic breakup in the reactions, the elastic cross sections have to be extracted from the data. The following procedure was used. The scattering angle distributions of protons detected in HiRA for both the inelastic and elastic peaks were extracted by applying a cut in the energy sum spectra at the junction between the two peaks. The elastic distributions were then obtained by subtracting the tail of the inelastic contamination leaking into the elastic peak above the junction, as determined from a double-Gaussian fit of the distributions (see Fig. 2). The resulting proton scattering angle distributions were then corrected for the geometrical acceptance of the HiRA array within its angular coverage, obtained from a Monte-Carlo simulation. The proton angular distributions obtained from the ^{9}C and ^{8}B elastic breakup events are shown in Fig. 3. There they are compared with the theoretical predictions from Continuum Discretized Coupled Channels (CDCC) calculations, that retain the full three-body final state kinematics of the target, residue (r) and the diffracted proton. The CDCC calculations make use of the methodology of Ref. [17] to calculate the laboratory frame multi-differential cross sections $d^3\sigma/d\Omega_r d\Omega_p dE_p$ of the proton and ^{8}B/^{7}Be residues that are then integrated over the angular acceptance ($\Delta\Omega_r$= 21 msr) of the fast, forward-going residue and all proton energies $E_p \leq 120$ MeV. The parameters used in the CDCC calculations are the same as employed for the earlier eikonal model results, including the complex proton-target and residue-target distorting potentials that were taken as the double- and single-folded interactions used to generate the corresponding eikonal elastic S-matrices. The unobserved cross section between 0° and 10° could be inferred from the excellent agreement between the CDCC theory and the observed distributions at larger angles. Percentages of unobserved cross section of 15(3)% and 28(5)% were calculated for the ^{9}C and ^{8}B elastic breakup cross sections, respectively,

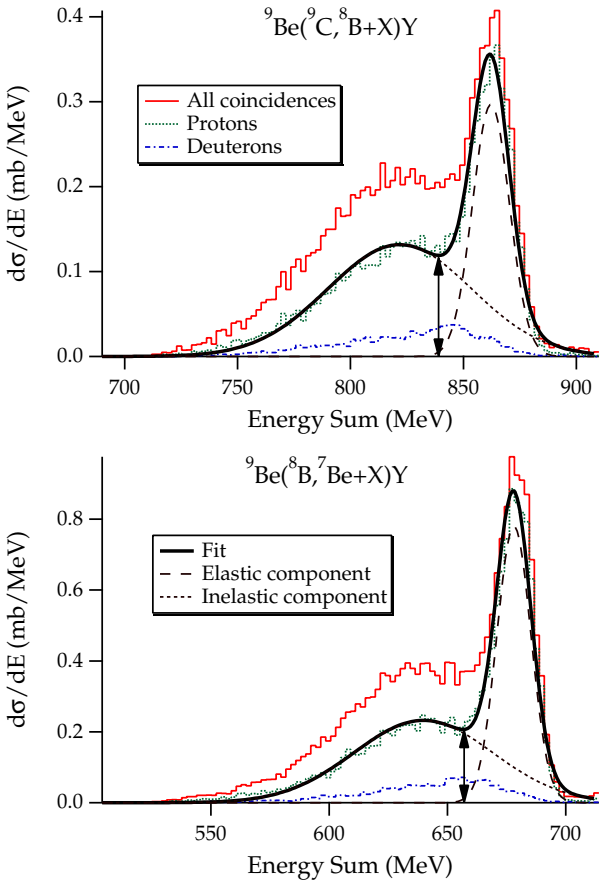

FIG. 2: (color online) Energy sum spectra of the one-proton knockout residue and the light particles detected in coincidence in the HiRA detector array for ^{9}C (top) and ^{8}B (bottom) projectiles. The sharp peak corresponding to elastic breakup is visible in proton coincidence events, whereas it disappears for deuteron and other inelastic coincidence events (see text). The inelastic and elastic components of the fit are shown, as well as the location of the cut indicated by the double arrow. The tail of the inelastic component leaking into the elastic peak amounts to 33% and 25% for the ^{9}C and ^{8}B breakups, respectively. The amount of elastic component leaking into the inelastic peak is negligible, due to the narrow width of the elastic peak.

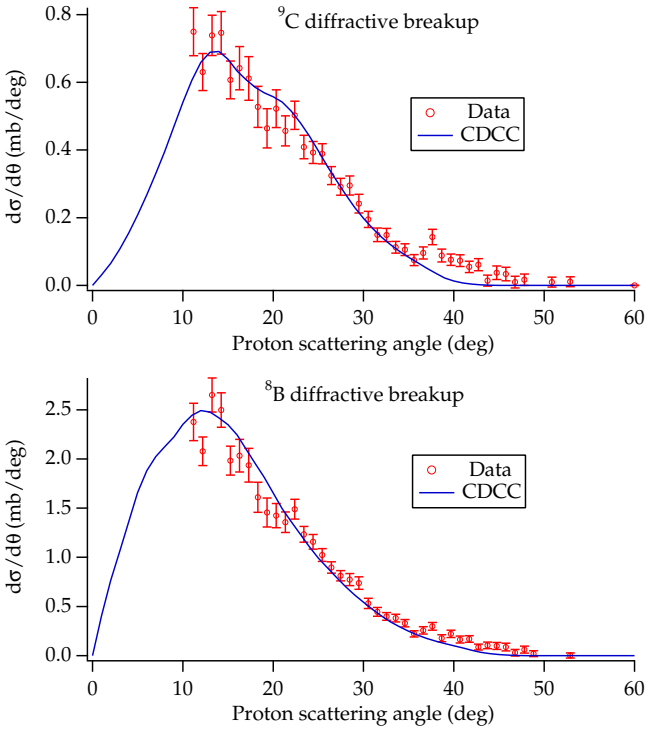

FIG. 3: Proton scattering angular distributions obtained for ^{9}C (top) and ^{8}B (bottom) elastic breakup events, after subtraction of the inelastic contamination using the fitted energy sum spectra (see Fig. 2). Also shown are the results from a CDCC calculation of the same quantity. The CDCC distributions are used to deduce the amount of unobserved cross section due to the lack of angular coverage between 0° and 10°, after (minor) normalization to the data.

using the CDCC distributions. The error bars on the corrections were determined from the minimum $\chi^2 + 1$ uncertainty band, by varying the amplitude of the CDCC cross sections until the reduced χ^2 relative to the data were increased by 1. After combining the data from the various magnetic rigidity settings necessary to cover the momentum distributions of the heavy residues, correcting for detector efficiencies and the finite angular acceptance of the S800, the integrated proton scattering angle distributions yielded cross sections of 13.8(6) mb and 49(2) mb for the elastic breakup cross sections of ^{9}C and ^{8}B respectively. The error bars include all contributions from the aforementioned analysis, the largest being the error on the correction due to the lack of angular coverage of the HiRA array between 0° and 10°.

The inclusive cross sections were obtained from the measured momentum distributions of the residues, for which no coincidence with the HiRA array was required. No corrections due to the limited angular acceptance of the HiRA array were therefore necessary. The cross sections were extracted by integrating the momentum distributions, following the procedure adopted in previous inclusive knockout reaction works (see for example [13]).

TABLE II: Measured and theoretical diffraction (including Coulomb) components of the one-proton knockout cross section for ^{9}C and ^{8}B. The calculated diffraction component agrees very well with the observation in both reactions. The large error bars in [14] come from the inclusive method used in that experiment. The theoretical inclusive cross sections are shown, which include center-of-mass correction factors $A/(A-1)$. The deduced reduction factors R_S=σ_{exp}/σ_{th} are also shown, as are the results from previous measurements.

Proj.	$\%_{diff}$ [a]	$\%_{diff}$ [b]	$\%_{diff}$ [14]	σ_{th} mb	R_S [a]	R_S [14]	R_S [9]
^{9}C	25(2)	26.8	26(10)	62.90	0.84(5)	0.82(6)	-
^{8}B	38(3)	37.1	28(14)	144.28	0.88(4)	0.86(7)	0.88(4)

[a] This work
[b] Calculated (from Table I)

The values obtained are 56(3) mb and 127(5) mb for the ^{9}Be(^{9}C,^{8}B)Y and ^{9}Be(^{8}B,^{7}Be)Y reactions, respectively. They are also in good agreement with the earlier results of Enders et al. [14].

In summary, our experiment has measured the elastic and inelastic components of the one-proton removal reaction cross section. Our extended proton detection geometry, which includes parts of the final-state phase-space where both the diffraction and stripping mechanisms contribute significantly, meant that the kinematic differences between the two reaction mechanisms were very apparent in the experimental data. Moreover, our analysis has shown that the observed diffraction and stripping contributions are very well reproduced by the eikonal model, as are shown in Table II. These results add considerable support to the use of the eikonal model as a quantitative tool, able, for example, to determine single-particle spectroscopic strengths in rare isotopes.

This work was supported by the National Science Foundation under Grant No. PHY-0606007, and the United Kingdom Science and Technology Facilities Council (STFC) under Grant No. EP/D003628.

* bazin@nscl.msu.edu

[1] P.G. Hansen and J.A. Tostevin, Annu. Rev. Nucl. Part. Sci. **53**, 219 (2003).
[2] T. Nakamura *et al.*, Phys. Rev. Lett. **96**, 252502 (2006).
[3] N. Fukuda *et al.*, Phys. Rev. C **70**, 054606 (2004).
[4] R. Palit *et al.*, Phys. Rev. C **68**, 034318 (2003).
[5] H. Simon *et al.*, Nucl. Phys. A **791**, 267 (2007).
[6] F. M. Marqués *et al.*, Phys. Lett. B **476**, 219 (2000).
[7] M. Zinser *et al.*, Nucl. Phys. A **619**, 151 (1997).
[8] R. Anne *et al.*, Nucl. Phys. A **575**, 125 (1994).
[9] B. A. Brown, P. G. Hansen, B. M. Sherrill and J. A. Tostevin, Phys. Rev. C **65**, 061601(R) (2002).
[10] D. J. Morrissey *et al.*, Nucl. Instrum. Methods Phys. Res. B **204**, 90 (2003).

[11] D. Bazin *et al.*, Nucl. Instrum. Methods Phys. Res. B **204**, 629 (2003).
[12] M. S. Wallace *et al.*, Nucl. Instrum. Methods Phys. Res. A **583**, 302 (2007).
[13] A. Gade *et al.*, Phys. Rev. C **69**, 034311 (2004).
[14] J. Enders *et al.*, Phys. Rev. C **67**, 064301(2003).
[15] B. A. Brown *et al.*, Prog. Part. Nucl. Phys. **47**, 517 (2001).
[16] M. Berz, K. Joh, J. A. Nolen, B. M. Sherrill, and A. F. Zeller, Phys. Rev. C **47**, 537(1993).
[17] J. A. Tostevin, F. M. Nunes and I. J. Thompson, Phys. Rev. C **63**, 024617 (2001).